The *in vivo* role of p38 MAP kinases in cardiac remodeling and restrictive cardiomyopathy

Pu Liao*†, Dimitrios Georgakopoulos†‡, Attila Kovacs§, Meizi Zheng*, Deborah Lerner§, Haiying Pu*, Jeffrey Saffitz¶, Kenneth Chien‖, Rui-Ping Xiao, David A. Kass‡, and Yibin Wang*††**

*Department of Physiology, University of Maryland School of Medicine, Baltimore, MD 21201; ‡Department of Medicine, Division of Cardiology, The Johns Hopkins Medical Institutes, Baltimore, MD 21287; Departments of §Medicine and ¶Pathology, Washington University School of Medicine, St. Louis, MO 63110; ‖University of California San Diego-Salk Program in Molecular Medicine, Department of Medicine and Center of Molecular Genetics, La Jolla, CA 92093; and **Laboratory of Cardiovascular Science, Gerontology Research Center, National Institute on Aging, National Institutes of Health, Baltimore, MD 21224

Edited by Eric N. Olson, University of Texas Southwestern Medical Center, Dallas, TX, and approved August 15, 2001 (received for review February 21, 2001)

Stress-induced mitogen-activated protein kinase (MAP) p38 is activated in various forms of heart failure, yet its effects on the intact heart remain to be established. Targeted activation of p38 MAP kinase in ventricular myocytes was achieved *in vivo* by using a gene-switch transgenic strategy with activated mutants of upstream kinases MKK3bE and MKK6bE. Transgene expression resulted in significant induction of p38 kinase activity and premature death at 7–9 weeks. Both groups of transgenic hearts exhibited marked interstitial fibrosis and expression of fetal marker genes characteristic of cardiac failure, but no significant hypertrophy at the organ level. Echocardiographic and pressure-volume analyses revealed a similar extent of systolic contractile depression and restrictive diastolic abnormalities related to markedly increased passive chamber stiffness. However, MKK3bE-expressing hearts had increased end-systolic chamber volumes and a thinned ventricular wall, associated with heterogeneous myocyte atrophy, whereas MKK6bE hearts had reduced end-diastolic ventricular cavity size, a modest increase in myocyte size, and no significant myocyte atrophy. These data provide *in vivo* evidence for a negative inotropic and restrictive diastolic effect from p38 MAP kinase activation in ventricular myocytes and reveal specific roles of p38 pathway in the development of ventricular end-systolic remodeling.

heart failure | conditional transgenesis

Heart failure evolving in response to sustained hemodynamic overload is among the most prevalent diseases in developed countries, particularly among the aged population (1). A commonly accepted paradigm for the development of failure divides the pathological process into two stages (2, 3). An initial compensatory stage is characterized by cardiac hypertrophy with preserved or even enhanced chamber systolic function and normal cardiac output. However, with persistently elevated loads, the heart evolves to a more decompensated state with contractile depression, myocardial fibrosis, and chamber stiffening (4). The underlying mechanisms for disease progression, including its initiation and transition to late-stage failure, and the molecular components mediating hypertrophic versus dilated or restrictive phenotypes remain poorly understood, but likely involve intracellular signaling pathways at different stages of its evolution (5).

The p38 subfamily of mitogen-activated protein (MAP) kinases has been shown to play an important role in mediating stress-induced signaling in mammalian cells (6). We and others recently reported that p38 MAP kinases were activated during development of hypertrophy and heart failure in response to pressure overload *in vivo* (7) and induced by ischemia/reperfusion in both animal and human hearts (8, 9). In cultured neonatal myocytes, activation of the p38 MAP kinase by MKK6bE leads to a hypertrophic response and cell survival, whereas expression of MKK3bE promotes an apoptotic response mediated through the p38α isoform (7, 10). Recent data from our laboratory further suggests that p38 activation mediates a negative inotropic effect in cultured adult rat cardiomyocytes (P.L., S. Wang, Y.W., and R.-P.X., unpublished results). These data suggest a potentially important role of p38 MAP kinases and selective signaling in the development of heart failure under pathological stresses (11). However, the *in vivo* effects of targeted p38 activation in intact hearts have not been studied, largely because of the difficulties of establishing transgenic animals with specific manipulation of p38 pathways in cardiomyocytes.

In this study, we established transgenic animals expressing the two well-established upstream activators of the p38 pathway (MKK3bE or MKK6bE) (12, 13) in ventricular myocytes to study the effects of p38 MAP kinase activation in the intact heart. A gene-switch approach was developed based on cre/loxP-mediated DNA recombination to restrict transgene expression to ventricular myocytes and avoid potential adverse effects of transgene expression on the survival of the founder transgenic animals (14–17). After the expression of MKK3bE and MKK6bE was genetically "switched on" in the ventricular myocytes, the resulting transgenic animals died prematurely from heart failure. Cardiac phenotypes induced by both p38 upstream activators shared several common features, including induction of hypertrophic marker gene expression and fibrotic remodeling in myocardium, systolic-contractile depression, and profoundly compromised diastolic function with increased chamber stiffness and restrictive chamber filling. However, striking differential effects on chamber remodeling and end-systolic wall stresses also were observed, with MKK3bE resulting in heterogeneous myocyte atrophy, end-systolic dilation, and wall thinning (higher stress), whereas MKK6bE resulted in mild myocyte hypertrophy with preserved or reduced cavity size. Our findings suggest that p38 MAP kinase signaling can contribute to the loss of contractility and myocardium stiffness and promotes specific remodeling process in heart failure. This study also demonstrates the utility of using gene-switch strategy to establish transgenic lines with early lethal phenotypes.

Materials and Methods

Transgenic Construct and Generation of Transgenic Animals. The schematic structure of the transgene constructs are shown in Fig. 1, and the details of their construction are published as supporting information on the PNAS web site, www.pnas.org. Activated mutants of human MKK3bE and MKK6bE, both hemagglutinin (HA)-tagged at the N terminal with substitution of Ser and Thr to Glu, have been described (12, 13, 18). Genotypes were screened by PCR on tail DNA as described in the supporting information.

Histological Analysis. Tissues were excised and fixed in 4% paraformaldehyde PBS for more than 4 h followed by dehydration

This paper was submitted directly (Track II) to the PNAS office.

Abbreviations: MAP, mitogen-activated protein; HA, hemagglutinin; GFP, green fluorescent protein; LV, left ventricle; MHC, myosin heavy chain.

†P.L. and D.G. contributed equally to this work.

††To whom reprint requests should be addressed. E-mail: ywang001@umaryland.edu.

The publication costs of this article were defrayed in part by page charge payment. This article must therefore be hereby marked "*advertisement*" in accordance with 18 U.S.C. §1734 solely to indicate this fact.

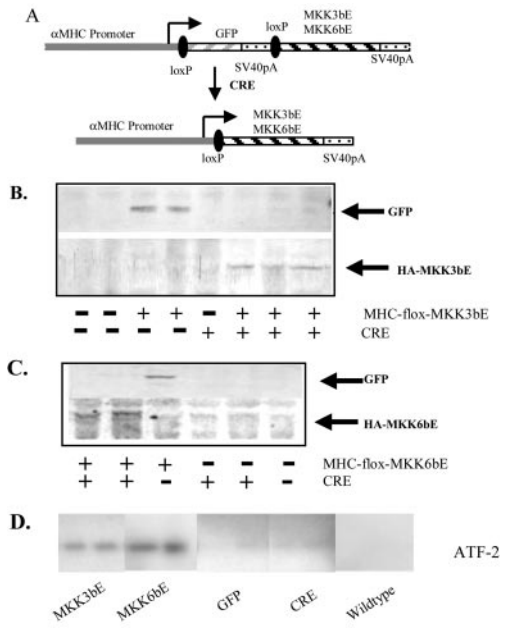

Fig. 1. Targeted expression of MKK3bE and MKK6bE in ventricular myocytes *in vivo*. (*A*) A schematic drawing of the transgene constructs used in the generation of floxed GFP/MKK3bE and floxed GFP/Mkk6bE transgenic mice (*Upper*) and resulting structure on *cre/loxP*-mediated DNA recombination in ventricular muscle cells after crossing with MLC-2v/Cre mice. (*B* and *C*) Representative Western blotting results for the expression of GFP, HA-MKK3bE/HA-MKK6bE recombinant proteins in mouse ventricles. The genotypes of the transgenic mice and their littermates are indicated at the bottom. −/− represents wild type; +/− and −/+ represent GFP-expressing MHC-flox-MKK3bE or MKK6bE- and CRE-expressing MLC-2v/cre single transgenic mice; +/+ represents MKK3bE- or MKK6bE-expressing double transgenic mice. (*D*) Representative autoradiograms of p38 kinase assays are presented. All samples were prepared from mice at similar age between 6 and 8 weeks.

and paraffin embedding and sectioning at 1 μm thickness. Hematoxylin/eosin staining was applied according to established protocols, and trichrome staining was performed as described by using a protocol modified from Masson's technique (19). Cross-sectional areas of myofilaments were measured by using Scion IMAGE (Frederick, MD) software on digitally recorded microscopic images from three hearts in each group, and the compiled data were presented by using SIGMAPLOT.

Protein, RNA Analyses, and Kinase Assay. Protein samples were prepared from snap-frozen hearts as described in the supporting information. Immunoblotting was performed by using anti-green fluorescent protein (GFP) antibody and anti-HA mAb (see supporting information). The p38 kinase assays were then performed at 30°C in the presence of [^{32}P] ATP using glutathione *S*-transferase-ATF2 as a substrate. RNA samples were prepared from the same heart tissues by using Trizol reagent (Life Technologies, Rockville, MD) according to the manufacturer's recommended protocol. The RNA dot-blot analysis was performed based on a published protocol (20) using a set of oligonucleotide probes. Reverse transcriptase–PCR were performed by using reagents from a Thermo-RT kit (GIBCO/Life Technologies). Details of these protocols and primer information are available as supporting information.

Hemodynamic Measurement. Six- to 7-week-old mice were anesthetized and ventilated before hemodynamic measurement (see supporting information). The pressure-volume catheter (Millar Instruments, Houston, TX) was inserted into the left ventricle (LV) chamber as detailed in the supporting information. Pressure-volume data were digitized at 2 kHz, and absolute volumes were calibrated as described (21). Resting hemodynamic parameters were determined from 6–10 digitally averaged cardiac cycles. Pressure-volume relations were obtained by transiently occluding the inferior vena as detailed in the supporting information.

Echocardiography. Noninvasive transthoracic echocardiograms were performed in conscious animals (Sequoia, Acuson, Mountain View, CA) as described (22). In echocardiography studies, all wild-type and Cre-positive single transgenic mice were grouped together as controls because MLC-2v/Cre mice have no detectable cardiac abnormalities (23).

Cell Contraction Measurement. Adult cardiomyocytes were isolated from rat hearts and infected with adenovirus vectors expressing MKK3bE, MKK6bE, and β-galactosidase as a control. Cell contraction was measured as described at room temperature under electrical stimulation (see supporting information).

Statistical Analysis. For hemodynamic and cell contraction studies, one-way ANOVA, with experimental groups (i.e., wild type, MKK3bE and MKK6bE, or control, Adv/lacZ, Adv/MKK3bE and Adv/MKK6bE) as the categorical variable was performed by using a Tukey's multiple comparisons test for posthoc testing of differences between groups. $P < 0.05$ was regarded as statistically significant. For echocardiography study, two-tailed Student's t test was performed between transgenic and nontransgenic littermate control groups.

Results

Targeted Activation of p38 Pathway in Ventricular Myocytes by Gene-Switch Transgenesis. Floxed transgenic lines were generated by using constructs containing murine α-myosin heavy chain (MHC) promoter driving GFP minigene flanked by two loxP sites, followed by another minigene expressing MKK3bE or MKK6bE mutant protein (floxed GFP mice, Fig. 1*A*). Two founder lines for the floxed-GFP MKK3bE mice and three founder lines for the floxed-GFP MKK6bE mice were obtained. GFP protein was detected in ventricular myocytes by fluorescent microscopy (data not shown) and Western blotting (Fig. 1 *B* and *C*). In contrast, the expression of HA-tagged MKK3bE or MKK6bE transgene products was not detected in these animals. These GFP-expressing transgenics developed normally with no significant cardiac phenotype (Figs. 7 and 8, which are published as supporting information). F_2 transgenic animals from line 53 of the floxed-GFP MKK3bE [GFP(MKK3bE)] mice and line 8 of the floxed-GFP MKK6bE [GFP(MKK6bE)] mice were used to breed with the MLC-2v/cre (Cre) heterozygous mice (24, 25) that have completely normal heart in morphology and function (ref. 23 and Figs. 7 and 8). In the double transgenic offspring that inherited both the MLC-2v/cre allele and the floxed-GFP transgene alleles (MKK3bE or MKK6bE mice), DNA recombination events between the two loxP sites resulted in the deletion of the GFP minigene sequences (data not shown). The consequent loss of GFP expression and the expression of MKK3bE or MKK6bE transgene was confirmed at protein level (Fig. 1 *B* and *C*), thus, a "gene switch" from GFP to the transgene was achieved in these hearts. Targeted expression of MKK3bE and MKK6bE proteins led to a significant increase in p38 kinase activities in the double transgenic ventricular myocytes compared to either single transgenic (Cre or GFPs) or wild-type control animals (Fig. 1*D*).

Pathological Remodeling in Morphology and Gene Expression of p38-Activated Transgenic Hearts. Activation of p38 MAP kinase activities in either MKK3bE or MKK6bE transgenic hearts led to premature death between 5 and 7 weeks of age with signs of dyspnea and pulmonary edema. Histological analysis revealed gross abnormalities in these double transgenic hearts compared to normal histology of the wild-type or CRE, GFP-expressing controls.

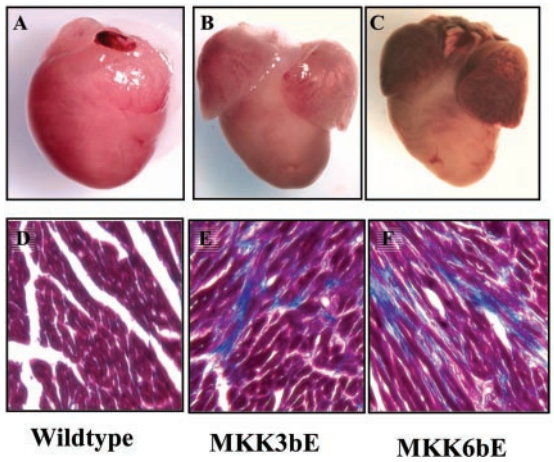

Fig. 2. Gross morphology of transgenic and wild-type control hearts (*A–C*) with indicated genotypes taken under the same magnification using a stereo dissecting microscope. Noting the enlarged atria in MKK3bE- and MKK6bE-expressing hearts but no significant changes in external sizes of the ventricles. (*D–F*) Trichrome staining of transgenic hearts with different genotypes as indicated. The fibrotic tissue is illustrated in dark blue. Noting the patchy staining pattern in both MKK3bE- and MKK6bE-expressing hearts, but absent in the wild-type control heart. (Magnifications: ×120.)

Both MKK3bE and MKK6bE hearts developed profoundly enlarged atria with increased atrial mass (Fig. 2, Table 1), which was often filled with thrombosis. However, external dimensions, right ventricle and LV mass and mass/body ratio were not significantly different from controls (Table 1). Both MKK3bE and MKK6bE transgenics displayed substantial interstitial fibrosis (Fig. 2). Associated with the morphological changes, expression of embryonic marker genes, including atrial natriuretic factor, β-MHC, and α-skeletal actin, were highly induced, whereas α-MHC, SERCA-2a (sarcoplasmic reticular calcium ATPase-2a), and phospholamban were down-regulated (Fig. 3). There were little differences in gene expression abnormalities between MKK3bE and MKK6bE transgenic groups. Such changes in expression profile are characteristic of cardiac failure in human and experimental models (20, 26–28), suggesting that activation of p38 MAP kinase pathways was sufficient to induce pathological changes at morphological and molecular levels as observed in failing heart.

Differential Chamber and Cellular Remodeling and Restrictive Filling in p38-Activated Transgenic Hearts. In contrast to histologic and gene expression analysis, M-mode echocardiography (Fig. 4, Table 2) revealed striking differences as well as similarities in intact chamber remodeling for the two transgenic models. Activation of p38 by MKK3bE resulted in left ventricular remodeling with increased end-systolic dimension but unchanged end diastolic dimension

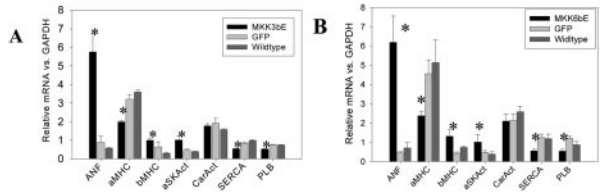

Fig. 3. Relative expression levels of cardiac marker genes measured by a dot blot method. The values are means of 4–6 samples from each genotype group and error bars represents standard errors. ANF, atrial natriuretic factor; aMHC, α-MHC; bMHC, β-MHC; aSKAct, α-skeletal actin; CarAct, cardiac actin; SERCA, sarcoplasmic reticular calcium ATPase-2a; PLB, phospholamban. *, $P < 0.05$ compared with wild-type or GFP control littermates.

(compared with control littermates), leading to a ≈20% decline in fractional shortening (Table 2). Echocardiography also showed that LV chamber dilation in MKK3bE hearts was associated with reduced wall thickness. In contrast, MKK6bE hearts had normal end-systolic cavity dimension, an ≈11% decline in LV end diastolic dimension, and preserved fraction shortening. Echocardiography revealed major similarities between models as well, including enlarged left atria that supported the histology data (Fig. 9, which is published as supporting information, and Table 2), and restrictive chamber filling (Fig. 4, Table 2), with increased peak E-wave velocity and rapid E-wave deceleration. Both findings suggested increased diastolic chamber stiffness in the transgenic hearts.

Further insight of differential effects of MKK3bE and MKK6bE on cardiac remodeling was provided by cellular histology. Although expression of MKK3bE in neonatal cardiomyocytes was previously shown to induce apoptosis, wall thinning in the MKK3bE heart was not associated with enhanced apoptosis as determined by terminal deoxyribonucleotide transferase-mediated dUTP nick-end labeling staining (data not shown). However, quantitative examination of MKK3bE heart cross sections revealed a marked dispersion of myocyte cross-sectional area, with more cells at a reduced size compared with controls, and a subpopulation of enlarged cells (Fig. 5). This finding suggested the presence of heterogeneous myocyte atrophy and sporadic hypertrophy in the MKK3bE heart that might contribute to the thinning of the chamber wall. In contrast, myocyte cross-sectional areas in MKK6bE hearts were slightly but significantly greater than controls. The presence of cellular hypertrophy in the MKK6bE transgenic heart may have contributed to the preservation of chamber end-systolic volume.

In contrast to early reports that documented a significant expression of both p38 α and β isoforms in cardiac tissue (29, 30), only p38α was detected at the protein level in the mouse heart whereas p38β was not detectable at either protein or mRNA levels (Fig. 10, which is published as supporting information). Therefore, the difference in cardiac phenotypes observed between MKK3bE and MKK6bE transgenic hearts is unlikely

PHYSIOLOGY

Table 1. Heart weight vs. body weight

Genotype	Wild type (n = 15)	GFP (n = 19)	MKK3bE (n = 12)	MKK6bE (n = 16)	ANOVA (vs. wild type)
BW (g)	22.0 ± 6.3 (n = 18)	20.5 ± 3.9 (n = 23)	19.9 ± 5.1 (n = 14)	17.4 ± 3.9* (n = 19)	0.04
RA (mg)	6.8 ± 2.6	7.5 ± 4.3	21.2 ± 7.6†	15.4 ± 9.3†	<0.0001
LA (mg)	7.7 ± 3.6	8.3 ± 6.4	26.7 ± 18.4†	46.2 ± 29.8†	<0.0001
LV (mg)	78.7 ± 17.0	93.7 ± 12.5	61.1 ± 23.7	93.6 ± 14.1	NS
RV (mg)	18.7 ± 5.7	17.7 ± 3.8	17.9 ± 4.3	17.2 ± 3.1	NS
LV/BW	3.7 ± 0.2	3.1 ± 0.1	3.1 ± 0.2	3.3 ± 0.2	NS
RV/BW	0.91 ± 0.08	0.89 ± 0.05	0.93 ± 0.06	0.96 ± 0.08	NS

All animals were between 6 and 7 weeks of age. Wild type and GFP were pooled littermates of MKK3bE and MKK6bE mice. BW, body weight; RA, right atrium; LA, left atrium; LV, left ventricle; RV, right ventricle. NS, not significant, $P > 0.05$.
*, $P < 0.05$ versus wild type.
†, $P < 0.005$ versus wild type and GFP.

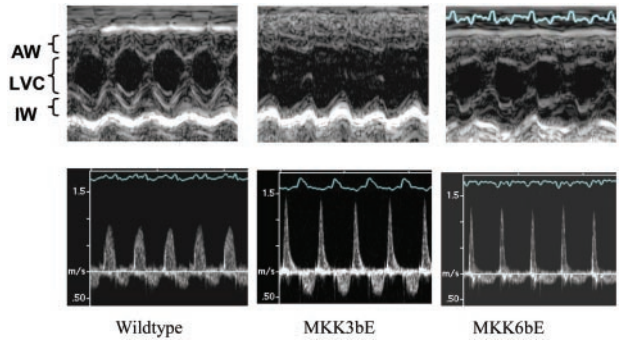

Fig. 4. Echocardiographic evaluation of cardiac structure and function in wild-type and transgenic mice. (*Upper*) Representative two-dimensional guided M-mode images of the LV demonstrate minimally increased relative wall thickness and minimally reduced fractional shortening in MKK6bE transgenic mice (both statistically nonsignificant) and significantly reduced relative wall thickness and fractional shortening in MKK3bE transgenic mice compared to wild-type control littermates. Of note, the steeper slope of endocardial motion during early diastole indicates an increased rate of wall thinning and LV chamber expansion in transgenic mice. AW, anterior wall; IW, inferior wall; LVC, left ventricular cavity. (*Lower*) Trans-mitral Doppler recordings show increased velocity and shortened deceleration time of early left ventricular filling and decreased isovolumic relaxation time in transgenic mice consistent with ''restrictive'' filling pattern and impaired left ventricular compliance.

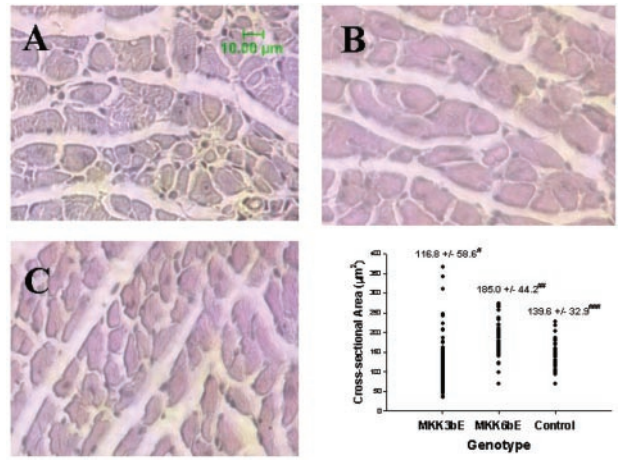

Fig. 5. Representative hematoxylin/eosin cross sections of LVs from MKK3bE (*A*), MKK6bE (*B*), and wild-type control (*C*) hearts. The cross-sectional areas (*D*) from individual myofilaments were complied with mean value ± SD for each group labeled at the top. *, $n = 198$; $P < 0.02$ vs. control; $P < 0.0001$ vs. MKK6bE. **, $n = 102$; $P < 0.001$ vs. control. ***, $n = 100$. Note the heterogeneous myocyte filament sizes in both hematoxylin/eosin section (*A*) and area measurement (*D*) from MKK3bE heart.

attributed to differential activities on p38α and β isoforms, but rather involves other downstream effectors.

Hemodynamic Assessment of p38-Activated Hearts. Left ventricular pressure-volume relations were obtained to more directly contrast systolic and diastolic chamber dysfunction in MKK3bE and MKK6bE transgenic hearts (Fig. 6, Table 3). These results confirmed similarities as well as some marked differences between transgenic mice expressing MKK3bE and MKK6bE versus littermate controls. Both transgenics had significantly reduced stroke volume (loop width), systolic pressure (loop height), and cardiac output, markedly elevated end-diastolic pressures, and a steeper diastolic pressure-volume curve (DPVR in Fig. 6). The latter confirmed passive diastolic stiffening consistent with the restrictive filling pattern revealed by Doppler analysis. Pressure-volume analysis independently confirmed major disparities in chamber volumes between the two models, with higher end-systolic volumes observed only in MKK3bE hearts and lower end diastolic volumes observed only in MKK6bE hearts. This remodeling was also demonstrated by V_{80}, the end-systolic volume at a matched end-systolic pressure of 80 mm Hg (Table 3). Although heart rate was somewhat slower in anesthetized transgenic animals versus controls, both mutant groups had similar rates so this observation could not explain disparities between them. Furthermore, this modest rate difference was out of proportion to the marked decline in cardiac output or ejection fraction. In addition to changes in chamber geometry and diastolic stiffening, both transgenic hearts displayed similar profound systolic depression, which was shown by an ≈40% decline in the peak rate of pressure rise (dP/dt_{max}), and nearly 60% decline in end-systolic elastance. In contrast to diastolic chamber stiffening, isovolumic pressure relaxation time constant (tau) was unchanged between control and transgenic animals. However, dP/dt_{min}, which is also influenced by end-systolic pressure differences, was less negative in the latter groups.

Negative Inotropic Effects of p38 Activation in Isolated Myocytes. To directly assess and compare the functional effects of different p38

Table 2. *In vivo* echocardiography analysis of transgenic hearts

	Control ($n = 6$)	MKK3bE ($n = 5$)	T test *P* value	Control ($n = 7$)	MKK6bE ($n = 7$)	T test *P* value
M-Mode						
HR, beats/min	644 ± 26	640 ± 38	NS	621 ± 19	605 ± 33	NS
LVPWd, mm	0.74 ± 0.05	0.53 ± 0.06	<0.0001	0.66 ± 0.07	0.67 ± 0.09	NS
IVSd, mm	0.77 ± 0.02	0.55 ± 0.04	<0.0001	0.72 ± 0.08	0.70 ± 0.09	NS
LVIDd, mm	3.12 ± 0.23	3.25 ± 0.30	NS	3.24 ± 0.11	2.87 ± 0.13	<0.0001
LVIDs, mm	1.43 ± 0.18	1.81 ± 0.32	<0.05	1.42 ± 0.12	1.36 ± 0.12	NS
FS, %	54.3 ± 2.9	44.2 ± 7.7	<0.05	56.2 ± 2.9	52.7 ± 2.7	NS
LAD	2.40 ± 0.12	3.67 ± 0.32	<0.0001	2.25 ± 0.21	3.66 ± 0.19	<0.05
Doppler						
HR, beats/min	640 ± 37	635 ± 54	NS	636 ± 41	602 ± 27	NS
E velocity, m/s	0.80 ± 0.06	1.20 ± 0.15	<0.0001	0.80 ± 0.09	1.31 ± 0.25	<0.001
E DT, ms	21 ± 1.8	9.0 ± 1.1	<0.0001	22 ± 0.9	11 ± 0.8	<0.0001
IVRT, ms	14 ± 1.3	8 ± 0.7	<0.0001	14 ± 0.8	9 ± 1.4	<0.0001

Echocardiographic measurements obtained transthoracic M-mode or Doppler tracings of transgenic hearts at ages between 6 and 9 weeks for MKK3bE and their littermate controls, and between 7 and 10 weeks for MKK6bE and their littermate controls, respectively. HR, heart rate: LV, left ventricle; LVPWd and IVSd, end-diastolic posterior wall and intraventricular septal thickness, respectively; LVIDd and LVIDs, end diastolic and end-systolic LV internal dimension, respectively; FS, fractional shortening (LVIDd-LVIDs/LVIDd); E, mitral E wave; DT, E wave deceleration time; IVRT, LV isovolumic relaxation time. *P* value, transgenic vs. corresponding control groups; NS, not significant between transgenic and corresponding control groups ($P > 0.05$).

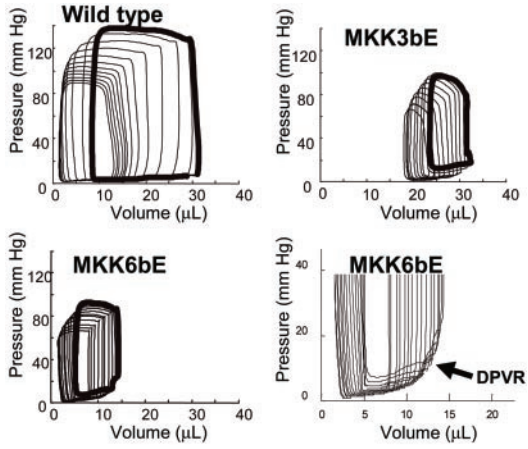

Fig. 6. Representative pressure-volume loops during basal (thick-line loop) and reduction of pre-load by vena cava occlusion (thin-line loops). MKK3bE-expressing hearts displayed a rightward shift of the end-systolic pressure-volume relation, whereas MKK6bE expressing hearts displayed a significantly leftward shift of the diastolic pressure-volume relation as compared with wild-type controls. (*Lower Right*) Reproduction of the diastolic relations on an expanded scale, demonstrating the marked increase in chamber passive stiffness measured in the MKK-expressing mutants. This example is from an MKK6bE animal, but very similar stiffening was measured in MKK3bE mice.

upstream activators on myocyte contractility, adult myocytes were isolated from rat hearts and infected with adenoviruses expressing MKK3bE, MKK6bE, or a marker gene *lacZ* as control, and cell shortening was studied 24 h later. Specific activation of p38 MAP kinase activities was achieved by adenovirus-mediated transgene expression in cultured myocytes (Fig. 11, which is published as supporting information), and resulted in profound systolic depression manifested by reduced cell shortening in both MKK3bE and MKK6bE expressing cells (44% and 62% relative to untreated controls, 50% and 71% relative to Adv-lacZ-infected cells, respectively, Table 4). Velocity of shortening and relengthening also declined, consistent with the reduced shortening magnitude. In agreement with *in vivo* observations (Table 3), both MKK3bE- and MKK6bE-infected cells displayed a similar extent of systolic depression.

Table 4. Contractility of isolated adult myocytes at 24 h after adenovirus transfection

Group	*n*	TA	V-Ls	V-Lr
Control	80	7.596 ± 0.466	−136.388 ± 9.959	129.450 ± 23.802
Ad-Lacz	59	6.699 ± 0.384	−104.068 ± 6.519*	89.356 ± 6.306
Ad-MKK3bE	76	3.880 ± 0.276†	−69.303 ± 3.725†	73.0395 ± 15.778‡
Ad-MKK6bE	41	4.686 ± 0.605†	−79.829 ± 9.7535§	66.366 ± 8.643¶

TA, Percent twitch amplitude. V-Ls, maximal velocity of shortening (μm/sec). V-Lr, maximal velocity of relaxation (μm/sec).
*, $P < 0.01$ vs control.
†, $P < 0.01$ vs. control and Ad-Lacz.
‡, $P = 0.05025$ vs. control.
§, $P < 0.01$ vs. control, $P < 0.05$ vs. Ad-Lacz.
¶, $P < 0.05$ vs. control and Lacz.

Discussion

We generated transgenic animals with targeted activation of p38 MAP kinases in ventricular myocytes by using a *cre/loxP*-based gene switch approach to express two activated mutants of upstream kinases for p38, MKK3bE and MKK6bE. In this article, we show that ventricular-specific expression of MKK3bE and MKK6bE proteins induced p38 MAP kinase activities in transgenic hearts, resulting in severe cardiomyopathy phenotypes with the following common features: (*i*) induction of hypertrophic marker gene expression and interstitial fibrosis; (*ii*) profound depression of systolic contractility; and (*iii*) compromised diastolic function with elevated chamber stiffness and restrictive filling. However, we also revealed substantial kinase-specific disparities in chamber remodeling—with end-systolic dilation, wall thinning, and myocyte atrophy observed only in MKK3bE-expressing hearts. This combination is striking, as it appears similar to that observed in the later stages of decompensation/remodeling in chronically overloaded ventricles. We have demonstrated a specific signaling pathway associated with overload has been shown to selectively generate this phenotype. In contrast, MKK6bE expressing hearts had reduced chamber volume accompanied by a mild increase in myocyte cross-sectional area, and thus had near normal end-systolic wall stress as compared with wild-type controls and MKK3bE hearts. Therefore, in addition to providing *in vivo* evidence for a substantial role of p38 MAP kinases in the development of both

Table 3. Hemodynamic measurement of transgenic mice and control animals

Measurement/genotype	Wild type ($n = 5$)	MKK3bE ($n = 7$)	MKK6bE ($n = 7$)	ANOVA (vs. wild type)
Systolic				
HR, beats per min	628.6 ± 20.9	528.0 ± 11.3*	545.8 ± 7.0*	<0.001
SV, μl	18.86 ± 1.32	10.68 ± 1.71*	8.55 ± 0.63*	0.0001
CO, ml/min	11.91 ± 0.86	5.71 ± 1.05*	4.66 ± 0.34*	<0.0001
EF, %	78.36 ± 3.05	42.15 ± 5.84*	50.21 ± 4.62†	0.0005
ESP, mmHg	108.9 ± 4.3	86.4 ± 4.7†	78.8 ± 3.4*	0.0006
dP/dt_{max}, mmHg/sec	15513 ± 717	8708 ± 502*	9073 ± 1203*	0.0002
Ees, mmHg/μl/100 mg	11.5 ± 0.82	5.7 ± 1.7*	3.6 ± 0.5*	<0.0001
V80, μl	3.1 ± 1.6	14.8 ± 0.41†‡	4.0 ± 1.8	0.003
Diastolic				
EDP, mmHg	8.50 ± 1.07	27.62 ± 1.86†	29.88 ± 1.58†	<0.0001
dP/dt_{min}, mmHg/sec	−12886 ± 474	−6286 ± 442*	−5890 ± 654*	<0.0001
Tau, msec	3.354 ± 0.116	3.803 ± 0.585	3.133 ± 0.428	NS
B100, per μl/100 gm $\times 10^{-3}$	8.8 ± 3.7	189 ± 19.4†	212 ± 46.9†	0.001

All animals were between 6 and 7 weeks of age. Wild types were pooled littermates of either MKK3bE or MKK6bE mice. HR: Heart rate, SV: stroke volume, CO: cardiac output, EF: ejection fraction, ESP: end-systolic pressure, dP/dtmax: maximum first derivative of pressure, EDP: end-diastolic pressure, dP/dtmin: minimum first derivative of pressure, Tau: time constant of isovolumic relaxation, Ees100: End-systolic elastance normalized to 100 mg LV weight, B: diastolic stiffness normalized to 100 mg LV weight, V80: end-systolic volume at common end-systolic pressure = 80 mmHg.
*, $P < 0.001$ vs. wild type.
†, $P < 0.01$ vs. wild type.
‡, $P < 0.01$ vs. MKK6bE.

systolic and diastolic cardiac failure, the present study identifies activator-specific remodeling effects concerning p38 pathway.

With sustained hemodynamic stresses, such as pressure overload or ischemia/reperfusion injury, prolonged activation of p38 could substantially contribute to reduced systolic function and exacerbate net cardiovascular limitations, accelerating the progression to overt failure. Although the underlying cellular and molecular mechanisms remain to be defined, several lines of evidence suggested the involvement of myofilament sensitivity to calcium, rather than calcium handling itself. For example, we have found that specific inhibition of p38 activity in cultured adult cardiomyocytes stimulates contractility by increasing intracellular pH without affecting calcium transients or membrane calcium currents, (P.L., S. Wang, Y.W., and R.-P.X., unpublished work). In intact hearts, unchanged tau in both MKK3bE and MKK6bE hearts supported the notion that calcium uptake during diastole was not affected despite the remarkable stiffness of the myocardium. Further studies will be needed to identify the molecular targets of p38 in cardiomyocytes that mediate the observed negative inotropic effect.

Although the exact downstream signaling for MKK3b versus MKK6b in cardiomyocytes remains unclear, prior studies have identified differences in the activation spectrum for p38 isoforms as well as different roles in other cellular functions independent of p38 (12, 31, 32). Our data revealed that p38α is the predominant isoform expressed in adult mouse hearts whereas p38β is not detectable at either protein or mRNA levels. Based on this and our cellular studies mentioned earlier, p38α and its downstream signaling events may play a major role in the development of common cardiomyopathy features in MKK3bE and MKK6bE transgenic hearts, including loss of contractility, myocardium stiffness, and changes in gene expression profile. On the other hand, the different forms of cardiac remodeling in MKK3bE and MKK6bE hearts could be mediated through different downstream effectors other than p38 as reported in the previous study (13). Activation of the MKK6b may be particularly important for preventing myocyte atrophy, achieving smaller cavity size and thus maintaining more normal or even reduced myocardial systolic stresses. This speculation would be consistent with data previously obtained in neonatal myocytes, revealing that hypertrophy and survival is preferentially mediated via MKK6bE instead of MKK3bE (7). Although there was a trend that MKK3bE had a stronger negative inotropic effect than MKK6bE on isolated myocytes (Table 4), the difference was modest and not statistically significant, and most likely would not account for the dramatic difference in chamber remodeling observed in intact hearts. Although we did not find evidence of apoptosis in MKK3bE animals, chamber wall thinning and relative dilation was associated with heterogenous reduction of myocyte cross-sectional area, suggesting that MKK3bE induced patchy myocyte atrophy in hearts, as often observed in end-stage failing human hearts. Therefore, the MKK6bE phenotype is more consistent with earlier phases of load-induced cardiac dysfunction—i.e., smaller chamber size, preserved end-systolic wall stress—whereas the MKK3bE phenotype is more characteristic of the later-stage decompensation. Such a correlation suggests that selective activation of p38 related pathways may indeed play an important role in this transition from compensated state to decompensated heart failure.

Transgenic approaches have implicated a variety of signaling pathways in the development of cardiac hypertrophy and heart failure, including G proteins, such as Gs (33), Ras (19), RhoA (34), and Gq (20), protein kinases (35) and phosphatases (27, 36), and cytokines (37). In transgenic animals with activated extracellular signal-regulated kinase (ERK) pathways induced by either Ras (19) or MAP kinase kinase (MEK) (38), massive cardiac hypertrophy developed in transgenic hearts. In contrast, activation of p38 in transgenic hearts led to minimal change in LV mass, suggesting that p38 MAP kinase signaling *in vivo* is not sufficient to induce hypertrophy, contrary to our own and other earlier *in vitro* reports based on studies in neonatal cardiomyocytes (7, 10). Based on this spectrum of *in vivo* phenotypes, we can hypothesize that the Raf-MEK-ERK pathway of the MAP kinases family may have an important role in the initiation of hypertrophy at the compensatory stages of the heart disease process, whereas p38 pathways may contribute to the loss of contractility and chamber remodeling at the transitional stages of heart failure. Further studies will be required to evaluate the efficacy of inhibiting p38 activities as a potential therapeutic approach to preserve contractility and prevent pathological remodeling in diseased hearts.

We acknowledge technical assistance from Dr. Bin Wu (University of Maryland), Ms. Julie Sheridan and Ms. Janelle Stricker (University of California, San Diego), and helpful discussion with Dr. J. Han (The Scripps Research Institute) and Dr. Joan Heller Brown (University of California, San Diego). This work was supported in part by National Public Health Service Grants HL61505–01 (to K.C.), HL59408 (to D.A.K. and D.G.), HL61505–01 and HL62311–01 (to Y.W.), and an Intramural grant from University of Maryland School of Medicine (to Y.W.).

1. Cohn, J. N., Bristow, M. R., Chien, K. R., Colucci, W. S., Frazier, O. H., Leinwand, L. A., Lorell, B. H., Moss, A. J., Sonnenblick, E. H., Walsh, R. A., *et al*. (1997) *Circulation* **95,** 766–770.
2. Grossman, W. (1980) *Am. J. Med*. **69,** 576–584.
3. Chien, K. R. & Grace, A. A. (1997) in *Heart Disease*, ed. Braunwald, E. (Saunders, Philadelphia), pp. 1626–1649.
4. Parmley, W. W. (1992) *Clin. Cardiol.* **15,** Suppl. 1, I5–I12.
5. Chien, K. R. (1999) *Cell* **98,** 555–558.
6. Ono, K. & Han, J. (2000) *Cell Signalling* **12,** 1–13.
7. Wang, Y., Huang, S., Sah, V. P., Ross, J., Jr., Brown, J. H., Han, J. & Chien, K. R. (1998) *J. Biol. Chem.* **273,** 2161–2168.
8. Bogoyevitch, M. A., Gillespie-Brown, J., Ketterman, A. J., Fuller, S. J., Ben-Levy, R., Ashworth, A., Marshall, C. J. & Sugden, P. H. (1996) *Circ. Res.* **79,** 162–173.
9. Cook, S. A., Sugden, P. H. & Clerk, A. (1999) *J. Mol. Cell. Cardiol.* **31,** 1429–1434.
10. Zechner, D., Thuerauf, D. J., Hanford, D. S., McDonough, P. M. & Glembotski, C. C. (1997) *J. Cell Biol.* **139,** 115–127.
11. Force, T., Pombo, C. M., Avruch, J. A., Bonventre, J. V. & Kyriakis, J. M. (1996) *Circ. Res.* **78,** 947–953.
12. Han, J., Lee, J. D., Jiang, Y., Li, Z., Feng, L. & Ulevitch, R. J. (1996) *J. Biol. Chem.* **271,** 2886–2891.
13. Huang, S., Jiang, Y., Li, Z., Nishida, E., Mathias, P., Lin, S., Ulevitch, R. J., Nemerow, G. R. & Han, J. (1997) *Immunity* **6,** 739–749.
14. Rajewsky, K., Gu, H., Kuhn, R., Betz, U. A., Muller, W., Roes, J. & Schwenk, F. (1996) *J. Clin. Invest.* **98,** 600–603.
15. Orban, P. C., Chui, D. & Marth, J. D. (1992) *Proc. Natl. Acad. Sci. USA* **89,** 6861–6865.
16. Lakso, M., Sauer, B., Mosinger, B., Jr., Lee, E. J., Manning, R. W., Yu, S. H., Mulder, K. L. & Westphal, H. (1992) *Proc. Natl. Acad. Sci. USA* **89,** 6232–6236.
17. Agah, R., Frenkel, P. A., French, B. A., Michael, L. H., Overbeek, P. A. & Schneider, M. D. (1997) *J. Clin. Invest.* **100,** 169–179.
18. Han, J., Wang, X., Jiang, Y., Ulevitch, R. J. & Lin, S. (1997) *FEBS Lett.* **403,** 19–22.
19. Hunter, J. J., Tanaka, N., Rockman, H. A., Ross, J. J. & Chien, K. R. (1995) *J. Biol. Chem.* **270,** 23173–23178.
20. D'Angelo, D. D., Sakata, Y., Lorenz, J. N., Boivin, G. P., Walsh, R. A., Liggett, S. B. & Dorn, G. W., 2nd (1997) *Proc. Natl. Acad. Sci. USA* **94,** 8121–8126.
21. Georgakopoulos, D. & Kass, D. (2000) *Am. J. Physiol.* **279,** H443–H450.
22. Rogers, J. H., Tamirisa, P., Kovacs, A., Weinheimer, C., Courtois, M., Blumer, K. J., Kelly, D. P. & Muslin, A. J. (1999) *J. Clin. Invest.* **104,** 567–576.
23. Minamisawa, S., Gu, Y., Ross, J., Jr., Chien, K. R. & Chen, J. (1999) *J. Biol. Chem.* **274,** 10066–10070.
24. Chen, J., Kubalak, S. W., Minamisawa, S., Price, R. L., Becker, K. D., Hickey, R., Ross, J. J. & Chien, K. R. (1998) *J. Biol. Chem.* **273,** 1252–1256.
25. Chen, J., Kubalak, S. W. & Chien, K. R. (1998) *Development (Cambridge, U.K.)* **125,** 1943–1949.
26. Arber, S., Hunter, J. J., Ross, J., Jr., Hongo, M., Sansig, G., Borg, J., Perriard, J. C., Chien, K. R. & Caroni, P. (1997) *Cell* **88,** 393–403.
27. Molkentin, J. D., Lu, J. R., Antos, C. L., Markham, B., Richardson, J., Robbins, J., Grant, S. R. & Olson, E. N. (1998) *Cell* **93,** 215–228.
28. Hirota, H., Chen, J., Betz, U. A., Rajewsky, K., Gu, Y., Ross, J., Jr., Muller, W. & Chien, K. R. (1999) *Cell* **97,** 189–198.
29. Stein, B., Yang, M. X., Young, D. B., Janknecht, R., Hunter, T., Murray, B. W. & Barbosa, M. S. (1997) *J. Biol. Chem.* **272,** 19509–19517.
30. Jiang, Y., Chen, C., Li, Z., Guo, W., Gegner, J. A., Lin, S. & Han, J. (1996) *J. Biol. Chem.* **271,** 17920–17926.
31. Enslen, H., Raingeaud, J. & Davis, R. J. (1998) *J. Biol. Chem.* **273,** 1741–1748.
32. Enslen, H., Brancho, D. M. & Davis, R. J. (2000) *EMBO J.* **19,** 1301–1311.
33. Iwase, M., Bishop, S. P., Uechi, M., Vatner, D. E., Shannon, R. P., Kudej, R. K., Wight, D. C., Wagner, T. E., Ishikawa, Y., Homcy, C. J. & Vatner, S. F. (1996) *Circ. Res.* **78,** 517–524.
34. Sah, V. P., Minamisawa, S., Tam, S. P., Wu, T. H., Dorn, G. W., 2nd, Ross, J., Jr., Chien, K. R. & Brown, J. H. (1999) *J. Clin. Invest.* **103,** 1627–1634.
35. Bowman, J. C., Steinberg, S. F., Jiang, T., Geenen, D. L., Fishman, G. I. & Buttrick, P. M. (1997) *J. Clin. Invest.* **100,** 2189–2195.
36. Bueno, O. F., De Windt, L. J., Lim, H. W., Tymitz, K. M., Witt, S. A., Kimball, T. R. & Molkentin, J. D. (2001) *Circ. Res.* **88,** 88–96.
37. Kubota, T., McTiernan, C. F., Frye, C. S., Slawson, S. E., Lemster, B. H., Koretsky, A. P., Demetris, A. J. & Feldman, A. M. (1997) *Circ. Res.* **81,** 627–635.
38. Bueno, O. F., De Windt, L. J., Tymitz, K. M., Witt, S. A., Kimball, T. R., Klevitsky, R., Hewett, T. E., Jones, S. P., Lefer, D. J., Peng, C. F., *et al*. (2000) *EMBO J.* **19,** 6341–6350.